

NEW SPECTROSCOPIC METHODS FOR THE SIMULTANEOUS ESTIMATION OF FUNDAMENTAL ATMOSPHERIC PARAMETERS USING THE LINE DEPTH RATIOS

CHULHEE KIM¹, B.-K. MOON¹, AND I.-H. LEE¹

¹Division of Science Education, Institute of Fusion Science, Chonbuk National University, Chonju 561-756, Korea
E-mail : ckim@chonbuk.ac.kr, moonbk@chonbuk.ac.kr, nanainho@naver.com
(Received January 05, 2012; Revised February 06, 2012; Accepted February 23, 2012)

ABSTRACT

New methods are developed to estimate the effective temperature (T_e), surface gravity ($\log g$), and metallicity ($[A/H]$) simultaneously with the spectral line depth ratios. Using the model atmosphere grids, depth values are calculated for the wavelength range of 4000Å–5600Å for various temperatures, gravities, and metallicities. All possible different combinations of line depth ratios for different pairs of ratios are investigated. A graphical 3D figure is produced with X, Y, and Z axes corresponding to T_e , $\log g$, and $[A/H]$, respectively. By reading a cross point of two curves plotted by a connection of three parameters obtained from spectral line depth ratio pairs on each of the three projected planes, T_e , $\log g$, and $[A/H]$ are determined simultaneously. In addition, an analytical method is devised based on the similar algorithm developed for the graphical method. Our methods were applied to estimate the fundamental atmospheric parameters of the Sun and Arcturus.

Key words : stars: atmosphere — stars: fundamental parameters

1. INTRODUCTION

Knowledge of the fundamental atmospheric parameters of stars such as effective temperature (T_e), surface gravity ($\log g$), and metallicity ($[A/H]$) is essential in understanding the atmospheric properties of stars and stellar systems. These three parameters also form the basis for analyzing HR diagrams and investigating stellar evolution. Therefore, enormous efforts have been focused on determining these atmospheric parameters as precisely as possible for many years, and many different methods have been developed (see Kovtyukh and Gorlova 2000).

All methods can be classified as either photometric or spectroscopic. In the former, several different relationships between photometric indices and atmospheric parameters have been derived for different color systems and for different kinds of stars using the calibration. In the latter, the slope of the Paschen Continuum is used. Balmer jump and wings of modest-strength lines such as H_α are used for hot and cool stars respectively. Each method has its own advantages and disadvantages but the errors are about a few tenths to hundredths of degrees.

Gray (1989) proposed a spectroscopic method using the ratio of the depths of two lines having different sensitivity to temperature. This technique was adopted by other investigators, and used for giants, supergiants, Cepheids, F, G stars, and early type dwarfs where CI,

SiI, VI, and FeI lines were used with errors of about 4–30 K (for more details, see Kim 2006; and references therein).

The advantage of this method is that the blending effect is smaller than in the case of using the equivalent width due to the relative absence of uncertain contributions from uncertain line wing, the small effect from different rotations, turbulence line broadening and abundance, and the small influence from spectral resolution. Thus, this method is appropriate for investigating the temperature variation due to the rotation and non homogeneous surface, the cyclic temperature changes of variable stars, and precise temperature structure of photospheres.

Kim (2006) extended this method for the estimation of both temperature and surface gravity simultaneously. Using the Kurucz model and the SYN-SPEC package, the author produced all synthetic spectral lines for the wavelength region of 4000–5700Å with $T_e=6000\text{--}7750\text{K}$, $\log g=3.5, 4.0, \text{ and } 4.5$, and metallicity of $[A/H]=0.0$. Then, the depth-ratios for all line pairs were investigated and the author selected two and six depth-ratios appropriate for the surface gravity and temperature indicators, respectively.

Six grids with X- and Y-axes were plotted for the depth-ratios of surface gravity and temperature, respectively, for the simultaneous estimation of these two atmospheric parameters through interpolation. This method was applied to the spectrum of δ Scuti for the determination of its temperature and surface gravity simultaneously.

Corresponding Author: B.-K. Moon

Now, we tried to extend this method again to determine the three fundamental atmospheric parameters of T_e , $\log g$, and $[A/H]$ simultaneously. Usually T_e and $\log g$ are estimated for a certain metallicity value. Therefore, prior to determining T_e and $\log g$, metallicity should be estimated. This situation is the same for both photometric and spectroscopic methods. However, metallicity is actually one of the most difficult parameters to estimate. Therefore, although it would be very useful and effective if the three parameters of T_e , $\log g$, and $[A/H]$ could be determined simultaneously, no such attempt has yet been made except once.

Recently, Kim and Moon (2011) developed a method for determining the three parameters simultaneously for the *wby* photometric system. Using a graphical method, T_e and $\log g$ were determined for various different values of $[A/H]$ using model atmosphere grids with respect to $(b-y):c1$ and $(b-y):m1$ pair indices. Then, a 3D figure was produced in which the X, Y, and Z axes correspond to T_e , $\log g$, and $[A/H]$, respectively.

By reading a cross point of two curves formed by the connection of the three parameters obtained from $(b-y):c1$ and $(b-y):m1$, pair indices on each of the three projected planes, T_e , $\log g$, and $[A/H]$ were determined simultaneously. This new method was applied to a number of field dwarfs and giants.

In the present paper, on behalf of $(b-y):c1$ and $(b-y):m1$ pair indices, we adopted different spectral line depth ratios with respect to different wavelengths, i.e., each different photometric index corresponds to a ratio of different line depths.

2. DISCUSSION

Our main purpose is to determine three parameters, T_e , $\log g$, and $[A/H]$, simultaneously, so we have to select at least three different spectral line depth ratios. Following the similar method proposed by Kim (2006), we calculated all synthetic spectral lines for the wavelength region of 4000–5600Å, $T_e=4000$ –6250K, $\log g=3.5, 4.0, \text{ and } 4.5$, as well as $[A/H]=-1.0, -0.5, +0.0, -0.5 \text{ and } +1.0$, turbulent velocity $V_{tubl}=2$ km/s, rotational velocity $V_{rot}=10$ km/s, and resolution of 0.01Å, using the Kurucz (1993)'s SYNTHE code, line data from Kurucz (1993, 1995)'s data base, Hirata & Horaguchi (1995)'s line list, Morton (2000)'s, DREAM database (Biemont et al. 2002), the VALD database (Piskunov et al. 1995), Fuhr & Wiese (2006), and other sources.

The total number of calculated lines was almost 200,000, but about 130,000 strong lines (continuum normalized values < 0.8) were selected for further investigation. The depth ratios were calculated for all different combinations of different temperatures, gravities and metallicities. Among these, only those pairs where the depth ratios varied smoothly along different temperatures and surface gravities were selected. In or-

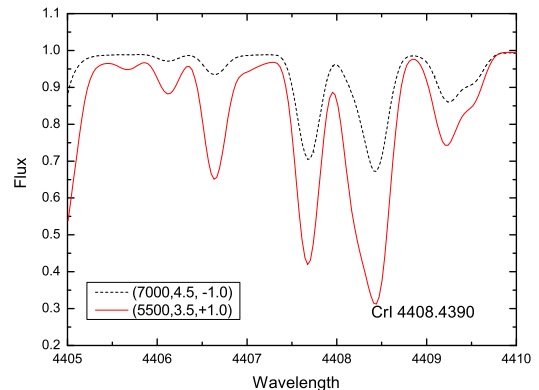


Fig. 1.— Synthetic spectra for different atmospheric parameters around CrI 4408.4390.

der to produce wider grids a further selection criterion was applied: the difference of the two ratios is larger than 0.1. As an example, Fig. 1 represents how the depth of line profiles can be changed along different atmospheric parameters. In this figure, dot and solid lines correspond to synthetic line profiles for various T_e , $\log g$, and $[A/H]$ of (7000:4.5:-1.0) and (5500:3.5:+1.0) respectively around CrI4408.4390Å.

The total number of final ratio pairs was 620 where the wavelengths were commonly identified for all four different metallicities. To plot a grid for a certain metallicity, we need two pairs of ratios. As an example, Table 1 presents the ratios for different T_e , $\log g$, and $[A/H]$. In this table, ratios for (TiI 4290.9238 / CrI 4337.5718) : (FeI 4006.6341 / FeI 4063.5820) as well as (TiI 4290.9268 / CrI 4337.5718) : (FeI 4408.4390 / FeI 4045.7981) correspond to two different pairs.

As an example of grids, Fig. 2 shows the model grids for the case of (TiI 4290.9238 / CrI 4337.5718) : (Fe I 4006.6341 / FeI 4063.5820) and (TiI 4290.9268 / CrI 4337.5718) : (FeI 4408.4390 / FeI 4045.7981) pairs for the X and Y axes respectively. Panel (a) shows four grids with different colours for $[A/H]=-0.5, 0.0, 0.5, \text{ and } +1.0$, and an asterisk corresponds to the position from the solar values

In panel (b), the region of the asterisk in panel (a) was enlarged to show the detailed grid structure. Each grid corresponding to a certain $[A/H]$ value occupies a different sector, and parts of the sectors are folded for $[A/H]=0.0$ and 0.5 and 1.0 However, for $[A/H]=-0.5$, the grids are placed on the far left side without folding by the other three cases. To be a good candidate for our purpose, the grid that contains a cross-point of two ratios in the X and Y axes should be folded for as many $[A/H]$ values as possible. A glance at the figure reveals that the overall grids move from the right to the left with increasing $[A/H]$ values.

Table 1.

Spectral line depth ratios from the Kurucz atmospheric models for different metallicity, temperature, and gravity values

		TiI 4290.9268 / CrI 4337.5718					FeI 4006.6341 / FeI 4063.5820			
		[A/H]					[A/H]			
log g	Te	-0.5	0	0.5	1	-0.5	0	0.5	1	
3.5	5500	1.0114	1.0304	1.0668	1.1173	5.2628	5.4041	5.0389	4.4365	
	5750	1.0947	1.1260	1.1757	1.2443	3.9024	3.8738	3.6380	3.3299	
	6000	1.1894	1.2335	1.2967	1.3773	2.9883	2.9550	2.8493	2.7164	
	6250	1.2895	1.3406	1.4150	1.5033	2.4415	2.4352	2.4084	2.3640	
4.0	5500	1.0097	1.0297	1.0678	1.1188	5.8101	6.1990	5.9003	5.0769	
	5750	1.0908	1.1228	1.1744	1.2443	4.5272	4.5800	4.2650	3.7594	
	6000	1.1813	1.2258	1.2928	1.3768	3.5159	3.4688	3.2539	2.9879	
	6250	1.2766	1.3297	1.4081	1.5030	2.7971	2.7618	2.6611	2.5333	
4.5	5500	1.0097	1.0335	1.0720	1.1235	6.1557	6.8422	6.8464	5.9807	
	5750	1.0913	1.1237	1.1779	1.2489	5.0416	5.3397	5.1085	4.4362	
	6000	1.1788	1.2239	1.2930	1.3801	4.0815	4.1315	3.8780	3.4346	
	6250	1.2691	1.3242	1.4057	1.5049	3.2860	3.2577	3.0681	2.8228	

		TiI 4290.9268 / CrI 4337.5718					FeI 4408.4390 / FeI 4045.7981			
		[A/H]					[A/H]			
log g	Te	-0.5	0	0.5	1	-0.5	0	0.5	1	
3.5	5500	1.0114	1.0304	1.0668	1.1173	3.9544	4.4387	4.7080	4.5014	
	5750	1.0947	1.1260	1.1757	1.2443	3.3924	3.6220	3.6379	3.3658	
	6000	1.1894	1.2335	1.2967	1.3773	2.8780	2.9270	2.8393	2.6341	
	6250	1.2895	1.3406	1.4150	1.5033	2.4293	2.4244	2.3522	2.2423	
4.0	5500	1.0097	1.0297	1.0678	1.1188	4.0596	4.5997	4.9476	4.7963	
	5750	1.0908	1.1228	1.1744	1.2443	3.6046	3.9320	4.0622	3.7745	
	6000	1.1813	1.2258	1.2928	1.3768	3.1816	3.3246	3.2636	2.9842	
	6250	1.2766	1.3297	1.4081	1.5030	2.7682	2.7947	2.6931	2.4880	
4.5	5500	1.0097	1.0335	1.0720	1.1235	4.2275	4.6853	5.1088	5.0610	
	5750	1.0913	1.1237	1.1779	1.2489	3.7439	4.1670	4.4370	4.2521	
	6000	1.1788	1.2239	1.2930	1.3801	3.4021	3.6756	3.7529	3.4653	
	6250	1.2691	1.3242	1.4057	1.5049	3.0802	3.2157	3.1479	2.8794	

Next, Te and log g are determined simultaneously using Table 1. As a test star, we adopted the Sun and tried to apply our methods to the estimation of three parameters for the Sun. Solar spectra and depth values were obtained from Hinkle et al. (2000), and the depth values for TiI 4290.9268, CrI 4337.5718, FeI 4006.6341, FeI 4063.582, FeI 4408.4390 and FeI 4045.7981 are 0.2107, 0.1701, 0.1992, 0.0527, 0.1714 and 0.0491, respectively. Hence, the ratios corresponding to (FeI 4290.9268/CrI 4337.5718), (FeI 4006.634/FeI 4063.5820), and (FeI 4408.4390/FeI 4045.7981) are 1.2387, 3.7799 and 3.4908 respectively. If we know the (X : Y) axes values from observed spectra, we can estimate the Te and log g simultaneously through an interpolation for each different metallicity following the method proposed by Kim (2006).

As an example for the Sun, the (X:Y) axes values correspond to the asterisk in Fig. 1, and the asterisk is commonly occupied by three grids corresponding to [A/H]=0.0, +0.5 and +1.0. However, a grid for [A/H]=-0.5 is not included, so this grid cannot be used which means that above four lines cannot be used to estimate Te and log g for [A/H]=-0.5. On the other hand, because the lengths of four sides of a certain grid are all different, simple one-dimensional interpolation is inadequate.

This is an exceptional case, in which two parameters should be determined from two variables simulta-

neously using the interpolation method. To do this, we devised a computer program with MATLAB that enabled simultaneous 2D interpolation. Finally, the estimated Te and log g values from the three grids corresponding to [A/H]=0.0, +0.5, and +1.0 are shown in Table 2. In Table 2, we can see that Te and log g are not available for [A/H]=-0.5, indicating that the ratios are out of the ranges in the model grids.

In the next step, we devised graphical and analytic methods to determine the metallicity simultaneously in addition to the two parameters of Te, and log g. To introduce the graphical method, Fig. 3 presents a 3D figure in which the X, Y, and Z axes correspond to Te, log g, and [A/H], respectively. The two thick red curves in the figure correspond to the three parameter values in Table 2 from (TiI 4290.9268 / CrI 4337.5718) : (FeI 4006.6341 / FeI 4063.5820) and (TiI 4290.9268 / CrI 4337.5718) : (FeI 4408.4390 / FeI 4045.7981) pairs in 3D space, and these two curves were projected on the (Te:[A/H]), ([A/H]:log g), and (Te:log g) planes with yellow, pink, and grey colors, respectively.

By reading a cross point of the two curves on each of the three projected planes, Te, log g, and [A/H] can be determined simultaneously. As an example, on the projected ([A/H]:Te) plane, [A/H] and Te values can be read from the position of a cross point of two curves through interpolation. Here we assumed that the result for two ratio pairs should be the same

Table 2.
Interpolated Te and log g values for different $[A/H]$ from the model grids.

(Ti I 4290.9268/Cr I 4337.5718): (Fe I 4006.6341/Fe I 4063.5820)			(Ti I 4290.9268/Cr I 4337.5718): (Fe I 4408.4390/Fe I 4045.7981)		
$[A/H]$	Te	log g	$[A/H]$	Te	log g
0.0	6034	4.30	0.0	6034	4.32
0.5	5883	4.03	0.5	5883	3.82
1.0	5746	3.96	1.0	5739	3.57

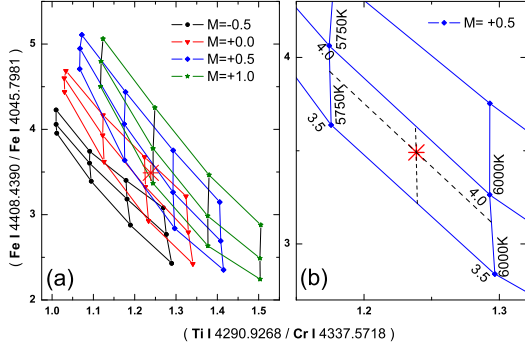


Fig. 2.— Atmospheric model grids for (Ti I 4290.9268/Cr I 4337.5718) and (Fe I 4408.4390/ Fe I 4045.7981) pairs for four different metallicities.

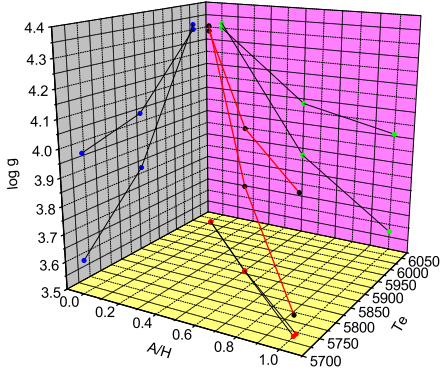


Fig. 3.— Simultaneous graphical estimation of Te, log g, and $[A/H]$ using the 3D plot.

for the same star if the synthetic spectra are appropriate for that star. Actually, each parameter can be determined twice, and the mean value was adopted. The results from the graphical method for the Sun are (0.42:5905), (6022:4.27), and (0.04:4.28) from the ($[A/H]$:Te), (Te:log g), and ($[A/H]$:log g) planes respectively, and the mean values of Te, log g, and $[A/H]$

are (5963:4.28:0.23), respectively. These results can be compared with the solar values of (5777:4.43:0.0).

Practically, the graphical approach is somewhat complicated and time consuming, so an analytic method was developed based on the graphical method. Although the principle of the two methods is equivalent, they are not identical and the results are somewhat different. For all metallicity values in the atmospheric grids, Te and log g are determined from a grid corresponding to (Ti I 4290.9268/Cr I 4337.5718): (Fe I 4408.4390/Fe I 4045.7981) through the same interpolation as in the graphical method. All Te and log g values are presented in the left part of Table 3, and these values are the same as those in the second and third columns in Table 3.

Then another grid corresponding to (Fe I 4290.9268 / Cr I 4337.5718) : (Fe I 4006.6341 / Fe I 4063.5820) can be plotted using Table 2. In the both grids, the X-axis is the same, but the Y-axis is different. If we mark the Te and log g values on the second grid with the same metallicity, we can read the Y-axis value corresponding to the marked point. All Y-axis values for different $[A/H]$ values are presented in Table 3. The Y-axis corresponds to the ratios for (Fe I 4408.4390/Fe I 4045.7981), and this ratio for the Sun is 3.78. Among the four ratios, the three values that are closest to this ratio of 3.78 (i.e., the observed solar ratio placed between the closest values that are smaller and larger than 3.78) can be read out.

In Table 3, the solar value of 3.78 is in between 3.80 and 3.62, so Te, log g, and $[A/H]$ should be within the values in Table 3 marked with underlines. Finally, Te, log g, and $[A/H]$ values can be determined through simultaneous interpolation to give results of [6008:4.23:+0.42], in comparison with [5963:4.28:+0.23] from the graphical method, respectively. The Te and log g values are not markedly different, but the $[A/H]$ values are too divergent.

Finally, as another test, our method was applied to Arcturus (K1.5III). Arcturus was selected because high resolution and high S/N ratio spectra are available, and the atmospheric parameter values have been accurately determined. Observed spectra was obtained from Hinkle et al. (2000). In order to apply our graphical method, the 3-D figures were plotted using those lines of Fe I 4000.398Å, Co I 4020.896Å, Sc I 4023.657Å, Ca I 4282.984Å, Fe I 4375.936Å, and Fe I 4647.426Å. Then all cross points on the projected planes were investigated,

Table 3.

The calculated ratios corresponding to (FeI 4006.6341/FeI 4063.5820) for different [A/H] values using model grids.

(TiI 4290.9268/CrI 4337.5718): (FeI 4006.6341/FeI 4063.5820)	[A/H]	0.0	0.5	1.0
Te		<u>6034</u>	<u>5883</u>	5739
log g		<u>4.32</u>	<u>3.82</u>	3.57
FeI 4006.634/FeI 4063.5820	Y-axis	3.80	3.62	3.48

and the result of (4428:1.71:-0.25) were obtained. This result can be compared with the published values of (4286:1.66:-0.52) by Ramirez & Allende Prieto (2011).

3. CONCLUSION

Two spectroscopic methods, one graphical and the other analytic, were developed to determine the three fundamental atmospheric parameters of Te, log g, and [A/H] simultaneously for the ranges of $-0.5 < [A/H] < +1.0$, $4000 < Te < 6250K$, and $3.5 < \log g < 4.5$ using the spectral line-depth ratios. These ranges were adopted because we tried to apply our methods to the estimation of three parameters for the Sun and Arcturus as test cases. Actually, our methods can be extended to any range of the three parameters. We could confirm that the three parameters of the Sun and Arcturus were successfully estimated through proper combinations of selected spectral lines by applying our method.

The two curves on the (Te:[A/H]), (Te:log g), or ([A/H] : log g) planes do not always intersect on all three planes in our graphical method. Nevertheless, the graphical method can still be applied if the intersection is available for at least one plane. Although the more versatile analytic method can be programmed and applied to many stars simultaneously, the graphical method remains superior because the analytic method is heavily dependent on the reliability of one ratio of pair values.

The advantage of our method is that three parameters can be determined simultaneously. In our method, only the depth of lines is used. However, depth of each line profile can be measured inaccurately for peculiar, abnormal, or weak lines. Hence, the reliability of parameter values obtained from the measurements of equivalent width which is widely used to study abundance pattern is higher. Except this case, our method can be competed with all other photometric or spectroscopic methods.

ACKNOWLEDGMENTS

This paper was (partially) supported by research funds of the Korea Research Foundation (KRF-2009-0070737). Lee was partially supported by Chonbuk National University. Moon was supported by the National Research Foundation of Korea(NRF) grant funded by the Korea government(MEST) (No. 2011-0027505).

REFERENCES

- Biemont, J., Palmeri, P., & Quinet, P. 2002, Database of Rare Earths At Mons University
- Fuhr, R., & Wiese, W. L. 2006, New Critical Compilations of Atomic Transition Probabilities for Neutral and Singly Ionized Carbon, Nitrogen, and Iron, *J. Phys. Chem. Ref. Data*, 35, 1669
- Gray, D. F. 1989, The Rotational Break for G Giants, *ApJ*, 347, 1021
- Hinkle, K. et al. 2000, Visible and Near Infrared Atlas of the Arcturus Spectrum, *Astron. Soc. of the Pacific*
- Hirata, R., & Horaguchi, T. 1995, Atomic Spectral Line List, SIMBAD Catalog VI/69
- Kim, C. 2006, Spectral Line-Depth Ratio as a Precise Effective Temperature and Surface Gravity Indicator for Warm Stars, *J. Korean Astron. Soc.*, 39, 125
- Kim, C., & Moon, B.-K. 2011, A Method for the Simultaneous Estimation of Atmospheric Parameters Using the Photometric Indices in the uvby Color System, *AJ*, 141, 118
- Kovtyukh, V. V., & Gorlova, N. L. 2000, Precise Temperatures of Classical Cepheids and Yellow Supergiants from Line-Depth Ratios, *A&A*, 358, 587
- Kurucz, R. L. 1993, CDROMs No. 1-18 (Cambridge, MA, Smithsonian Astrophys. Obs.)
- Kurucz, R. L. 1995, CDROM No. 23 (Cambridge, MA, Smithsonian Astrophys. Obs.)
- Morton, D. C. 2000, Atomic Data for Resonance Absorption Lines. II. Wavelengths Longward of the Lyman Limit for Heavy Elements, *ApJS*, 130, 403
- Piskunov, N., Kupka, F., Ryabchikova, T., Weiss, W., & Jeffery, C. 1995, VALD: The Vienna Atomic Line Data Base, *A&AS*, 112, 525
- Ramirez, I., & Allende Prieto, C. 2011, Fundamental Parameters and Chemical Composition of Arcturus, *ApJ*, 743, 135